AIMS Environmental Science

AIMS Environmental Science, 11(1): 1–20.
DOI: 10.3934/environsci.2024001
Received: 21 November 2023
Revised: 01 January 2024
Accepted: 09 January 2024
Published: 18 January 2024

http://www.aimspress.com/journal/environmental

Research article

The conversion and migration behavior of phosphorus speciation during pyrolysis of different sludges

Qianlan Li[1,2], Qingdan Wu[1,2], Xiaochen Zheng[1,2], Pengfei Wang[1,2], Dongsheng Zou[1,2], Fen Liu[1,2] and Zhihua Xiao[1,2,*]

[1] College of Environment and Ecology, Hunan Agricultural University, Changsha, Hunan, 410128, China
[2] Key Laboratory for Rural Ecosystem Health in Dongting Lake Area of Hunan Province, Changsha 410128, China

* **Correspondence:** Email: xiaozhihua@hunau.edu.cn, Tel: +8673184673603; Fax: +8673184673603.

Abstract: The study was enforced to probe the conversion and migration behavior of phosphorus speciation in sludge and the biochar received from pyrolysis of municipal sludge (MS), town sludge (TS), and slaughterhouse sludge (SS). This study creatively used fractionation of soil phosphorus to further differentiate speciation of phosphorus in three sludges (MS, TS, and SS). According to the x-ray diffraction (XRD) analysis and sequential extraction, the study proved the dependence of P speciation conversion on pyrolysis temperature and different types of raw sludge. The results of P-fractionation indicated that Ca-bound IP (Ca-IP) content in all biochars significantly increased at pyrolysis temperature of 350–800 °C, and the proportion of soluble and loosely bound IP (SL-IP), aluminum-bound IP (Al-IP), and Fe-bound IP (Fe-IP) of MS and SS decreased. The difference is that the Al-IP in the TS increased slightly as the pyrolysis temperature increased. Among the three kinds of sludge, the Olsen-P of TS is the lowest because the content of Olsen-P in sludge will decrease with the decrease of pH in the process of sewage treatment after acidification. In addition, XRD patterns of three sludges and biochar further confirmed the low crystallinity of $AlPO_4$ minerals. Through in-depth research on the environmental behavior of phosphorus, this study might additionally provide essential knowledge for the recovery and utilization of phosphorus in sludge.

Keywords: sludges; pyrolysis; phosphorus; speciation; biochars; minerals

1. Introduction

Sewage sludge is a necessary by-product of sewage disposal process, which will cause serious harm to the environment if not handled properly [1]. In China, about 60,000,000 tons of raw sewage sludge was generated in 2019 and the figure is expected to exceed 90,000,000 tons by 2025 (calculated according to 80% water content) [2,3]. Among various sewage sludge treatment technologies, pyrolysis is considered a valid alternative method, which can significantly reduce sludge bulk, destroy pathogenic bacterium in sludge, and transform the sludge into biochar, which was the high value-added carbonaceous materials for many purposes, such as soil improvement [4], carbon sequestration [5], and pollution reduction [6]. The application of biochar prepared from sludge as a soil conditioner in improving the properties of urban soil and promoting grassland growth has been reported [7]. It was also shown that the use of biochar prepared from sludge as a soil conditioner plays an important role in stabilizing metal ingredients [8,9], attenuating phenanthrene/pyrene adsorption [10], and reducing the bioavailability of polycyclic aromatic hydrocarbons (PAHs) [11].

Sewage sludge usually contains 2-3% dry mass phosphorus [12], which makes the biochar derived from it a potential fertilizer in the process of soil application [13,14] but also a potential threat to the environment if not handled properly. The pyrolysis of sludge affects the content and speciation of phosphorus in the solid residues [15,16]. Pyrolysis can decompose organophosphorus compounds into inorganic phosphorus compounds. Organophosphate compounds are compounds containing carbon-phosphorus bonds, such as organophosphate esters and organophosphate anhydrides. The carbon-phosphorus bonds of these organophosphorus compounds break after pyrolysis, producing inorganic phosphorus compounds such as phosphate and phosphoric acid. These inorganic phosphorus compounds can be absorbed and utilized by plants in the soil, which plays a role in promoting plant growth [17]. Relevant studies have shown that the mobility and bioavailability of phosphorus are closely related to the speciation of phosphorus [18,19]. In-depth understanding of phosphorus speciation is necessary to understand the fate of phosphorus. On one hand, the utilization of biochar prepared by pyrolysis of sludges as soil conditioner or fertilizer requires plant-available phosphorus, but it is easily released. On the other hand, its use in building materials requires its fixation, because once excessive P is released into the water [20,21], it will cause eutrophication. Qin et al. [22] also reported that in most large lakes, phosphorus reduction can mitigate eutrophication, but in eutrophication lakes, especially shallow lakes (or bays), both nitrogen and phosphorus reduction may be required. Therefore, when the biochar is completely applied to the soil or building materials and so on, it is important to fully understand the behavior of the transformation and conversion of P in the biochar during thermal treating of the sewage sludge.

The speciation of phosphorus in sewage sludge and sludge biochar has engaged the consideration of researchers and has been reported in some existing studies. Based on sequential fractionation, Qian and Jiang [23] reported the transplantation of phosphorus operating form to the middle and long-term plant-absorbable phosphorus pool in sludge biochar provided at high

temperature. When sludge biochar is applied to the soil, it is necessary to understand the conversion and transplantation of phosphorus in the sludge during the pyrolysis process. Some research reports the delivery and preservation of phosphorus depends on its chemical speciation and its combined metal ions [23,24]. McDowell et al. [25] showed that the removable phosphorus speciation are the solvable phosphorus speciation that are infirmly assembled on Fe, Al, and Ca. Sharpley et al. [26] found that the conversion of phosphorus combined with Al, Fe, and Ca leads to a reduction in water-soluble phosphorus in the soil.

Understanding the speciation of phosphorus in sludge biochar is essential for understanding the fate of phosphorus, which helps predict the potential pollution of sludge biochar in the environment. However, little is known about the influence of pyrolysis temperature and different sludges on phosphorus chemical speciation conversion and transplantation of sludge biochar during pyrolysis. Moreover, previous studies have only focused on the standards, measurements, and testing (SMT) agreement for P speciation classification into total phosphorus (TP), inorganic phosphorus (IP), organic phosphorus (OP), non-apatite inorganic phosphorus (NAIP), and apatite inorganic phosphorus (AP)，ignoring the speciation of inorganic phosphorus combined with metal ions. From the above considerations, this study creatively used the fractionation of soil phosphorus according to [27] to differentiate among soluble and loosely bound IP (SL-IP), aluminum-bound IP (Al-IP), Fe-bound IP (Fe-IP), oxide occluded IP (O-IP), and Ca-bound IP (Ca-IP). Only by systematically studying the migration and transformation of phosphorus in sludge at different pyrolysis temperatures can we understand the impact of phosphorus on environmental pollution. Therefore, the objectives of this work were: (1) to compare the phosphorus transformation of three different sludge during pyrolysis (200800 °C) process and (2) to conclude the bioavailability and chemical properties of phosphorus speciation of sludges and their biochar determined by fractionation of soil phosphorus and X-ray diffraction analysis.

Phosphorus speciation of sewage sludges after microwave-assisted pyrolysis or incineration has been reported in literature [28,29], but little research has compared phosphorus speciation of different sludges and their biochar. The research reported here was undertaken to compare and contrast the conversion and migration behavior of phosphorus speciation of different sludges after pyrolysis. Through the in-depth discussion of the experimental results of phosphorus morphology, this study deduced the possible phosphorus phase and provided an important explanation for the phosphorus migration during the application of sludge and biochar prepared from its in soil. In this study, the morphology of phosphorus was explained in depth, which provided a foundation for further study on the conversion and transplantation of phosphorus morphology during sludge pyrolysis.

2. Materials and methods

2.1. Materials collection and pre-treatment

Three typical of sewage sludge were selected in this study: municipal sludge (MS), town sludge (TS), and slaughterhouse sludge (SS). MS and SS were gathered in two diverse sewage disposal plants in Changsha, China. They differ from the efficiency of phosphorus removal (chymic

phosphorus-sediment and enhanced biological phosphorus-removal) and the subsequent processing of sewage sludge (aerobic and anaerobic steadiness). The municipal sewage disposal plant was in a first step biological precipitation and aerobic stabilization, and the next step is flocculant precipitation. The flocculants are mainly used for sludge dewatering in sewage plants, which can change the physicochemical property of sludge particles, undermine the colloidal structure of sludge, reduce the affinity of sludge particulate and water, and build up the dehydration property of sludge accordingly. The slaughterhouse sludge was contemporaneously precipitated with $FeCl_2$ and then rapidly fermented to form anaerobic stable sludge. TS was gathered from a rural sewage disposal plant in Dongguan city, China. The sewage disposal plant mainly collects household sewage, some industrial effluents, and overland runoff. Therefore, TS from this plant involved a lot of inorganic matter, containing heavy metals and deposit sediment. The plant adopted circulating activated sludge technology for sewage disposal. The circulating activated sludge system is composed of anoxic selector, pre-reaction aerobic zone, main aerobic reactor, etc. Unlike municipal sludge and slaughter sludge, hydrogen peroxide is added to the TS to form Fenton reagent, oxidation by hydrogen peroxide at acidic conditions dissolve bacterial cells and waste-activated sludge composed of extracellular polymeric substances, promoting the subsequent sludge dewatering. All samples were dried in an oven at 105 °C for 24 hours to ensure that the moisture content was less than 1%. Then, the dried sample was crushed and sieved into fractions of particle diameter 80–200 meshes.

2.2. Pyrolyzer and pyrolysis process

A lab-scale pyrolysis device (SK-G08123K, China) was used in this pyrolysis experiment. The pyrolysis device used in this study is the same as the previous study [30]. Municipal sludge, town sludge and slaughterhouse sludge were utilized for laboratory scale pyrolysis experiments. Specific pyrolysis process was refer to Shao et al. [30]. The pyrolysis temperatures were 200 °C, 350 °C, 500 °C, 650 °C, and 800 °C, the heating rate was 10 °C min^{-1}. Pyrolysis temperatures were sustained for 30 minutes.

The biochars produced from MS, TS, and SS at various temperatures (200 °C, 350 °C, 500 °C, 650 °C, and 800 °C) were designated as follows: MS200, MS350, MS500, MS650, MS800; TS200, TS350, TS500, TS650, TS800; and SS200, SS350, SS500, SS650, SS800, respectively. The resulting biochars were stored in a dryer at an indoor temperature for subsequent use.

2.3. Analytical procedures

2.3.1. Physicochemical analysis

For the methods of ultimate composition and proximate analysis of sludges and corresponding biochars, refer to Zeng et al. [31]. Mineral phases of sludges and corresponding biochars were identified by X-ray diffraction (XRD) measurement.

2.3.2. Sequential extraction

Total P (TP) and inorganic P (IP) concentrations were analyzed by the ignition approach [32]. The TP content was analyzed by igniting a 1.0 g manure or biochar at550 °C for 1 hr and then

extracting with 25 mL 0.5 mol L^{-1} H_2SO_4 for 2 h. The IP concentration was analyzed by the same extraction routine. We centrifuged at 4000 RPM for 20 minutes to separate the liquid from the solid phase. The supernatant liquid was then filtered through a 0.45 μm membrane filter and the P concentration was measured by the molybdenum blue method [33]. The organic P (OP) concentration was figured as the difference between TP and IP.

The IP fractions were separated using the fractionation of soil phosphorus [27] and soil agrochemical analysis method. Soil inorganic P can be further classified into different fractions, such as soluble and loosely bound IP (SL-IP), aluminum-bound IP (Al-IP), Fe-bound IP (Fe-IP), oxide occluded IP (O-IP), and Ca-bound IP (Ca-IP). Although there are some reports of deficient extraction of Al-P and Fe-IP fractions [34], this method can adequately distinguish these fractions. The above-mentioned P-fraction was extracted with different extraction agents.

Step 1: soluble and loosely bound IP (SL-IP) was extracted with 50 ml of 1.0 mol L^{-1} NH_4Cl. Step 2: aluminum-bound IP (Al-IP) was extracted with 50 ml volume of 0.5 mol L^{-1} NH_4F (pH8.2). Step 3: Fe-bound IP (Fe-IP) was extracted with 50 ml volume of 0.1 mol L^{-1} NaOH. Step 4: Oxide occluded IP (O-IP) was extracted with 40 mL 0.3 mol L^{-1} $Na_3C_6H_5O_7$ and 1.0 g $Na_2S_2O_4$. Step 5: Ca-bound IP (Ca-IP) was extracted with 50 mL of 0.25 mol L^{-1} H_2SO_4. The specifics of extraction method was reported previously [35]. Each experiment was conducted in quadruplicate.

2.4. Characteristic of raw sludges and their biochar

The contents of volatile matter, fixed carbon, and ash (proximate analysis) of the MS, TS and SS (on dry matter basis) and the ultimate compositions (ultimate analysis) of MS, TS, and SS were revealed in Table 1. The outcomes of proximate analysis and ultimate analysis revealed that the volatile matter and the fixed carbon were as high as 58.74 % and 12.11% in SS and the content of ash was 29.15%. But, for MS, the content of carbon was 3.56% and the ash reached up to 54.12%. Meanwhile, the percentages of ash was the highest and the contents of fixed carbon and volatile matter were the lowest in TS. This illustrates the complexity of sludge and the multiplicity of its components. Moreover, the contents of C, H, and N of MS were the highest and the contents of C, H, O, and N of TS and SS were very similar. The difference in element composition can be illustrated by the difference in the catchment area of the sewage disposal plant.

Table 1. Properties of MS, TS, and SS.

Items	Proximate analysis [a] (wt %)			Elemental analysis (wt %)				
	VM	Ash	FC	N	C	H	S	O [b]
MS	42.32	54.12	3.56	5.25	24.73	3.62	0.61	65.79
TS	29.02	68.31	2.67	2.76	15.48	2.98	0.73	78.05
SS	58.74	29.15	12.11	2.98	18.87	2.06	0.27	75.82

Notes: VM: volatile matter; FC: fixed carbon, [a] Dry basis, [b] Calculated by difference, (O = 100 - (C + H + N + S)).

3. Result and discussion

3.1. Total concentration of Phosphorus and residual rate of Phosphorus in biochar during pyrolysis

The total concentrations of phosphorus in sludges (MS、TS, and SS) and biochars pyrolyzed by sludges (MS, TS, and SS) were revealed in Table 2. Among the three types of raw sludge, TS has the highest total phosphorus contents, followed by MS, and SS has the lowest total phosphorus concentration. TS has a higher P-concentration compared to MS and SS, which can be illustrated by the differences between the catchment areas of the the sewage disposal plants [36]. The sewage disposal plants of MS and SS have a more industrial catchment area, while the sewage disposal plant of TS is in a more rural area.

Table 2. Contents of total phosphorus in the sludge and the biochar and residual rate of phosphorus in biochar.

Temperature	MS		TS		SS	
	contents (mg g^{-1})	Ratios (%)	contents (mg g^{-1})	Ratios (%)	contents (mg g^{-1})	Ratios (%)
Sludges	12.5	/	19.64	/	9.70	/
200	13.86	99.10	21.90	98.70	11.01	99.24
350	19.89	94.84	23.91	97.89	17.07	99.61
500	24.46	93.10	25.24	96.16	19.56	95.87
650	21.93	79.49	22.14	81.65	18.66	87.31
800	22.72	77.11	22.54	81.01	18.15	80.24

All biochars prepared from sludge showed expressively increased TP content with increasing pyrolysis temperature where TP promoted from 12.5 mg/g in MS to 22.72 mg/g in MS800, 19.64 mg/kg in TS to 22.54 mg/g in TS800, and 9.70 mg/g in SS to 18.15 mg/g in SS800. This may be caused by the decomposition of organic components in the sludge [37]. TP recovery showed that a large proportion of the P was reserved in the biochar with recovery percentages as follows: 77.11–99.10% in MS biochar, 81.01–98.70% in TS biochar, and 80.24–99.61% in SS biochar. When the pyrolysis temperature ranges from 200 ℃ to 500 ℃, there is no significant difference in the recovery rate of TP. When the pyrolysis temperature ranges from 650 ℃ – 800 ℃, the TP recovery rate decreased slightly. The higher phosphorus recovery percent indicates that the phosphorus involved in bio-oil or gas was expressively shallower than that in biochar. The results are identified with fore works, which recovered almost all P speciation from biochar [38]. As the pyrolysis process progresses, part of the oxygen and hydrogen, as well as nitrogen and sulfur, are lost in the feedstock, thereby enriching the remaining P into the biochar [39,40]. These results indicate that phosphorus can be recycled or reused through the pyrolysis of organic waste. P mainly remains in the solid residues, and its distribution in the liquid and gas phase is restricted. The relative fractions of P in solid phase, liquid phase, and gas phase are in connection with the type of raw material, P speciation, and processing circumstances (mainly temperature). For instance, when the pyrolysis temperature is 250–600 °C, P recovery in the solid residues is about 80% for wheat straw, about 100% for maize straw and peanut husk, and about 100% for sewage sludges and manures [41].

3.2. Influence of pyrolysis temperature on the phosphorus speciation.

The total concentrations and recovery of different speciation of phosphorus in sludges (MS, TS, and SS) and biochars pyrolyzed by sludges (MS, TS, and SS) were revealed in Table 3. The total phosphorus content in TS was the highest while that in SS was the lowest. All biochars showed significantly decreased organic phosphorus (OP) content with increasing pyrolysis temperature where OP reduced to 6.96 mg/g in MS200 to 0.61 mg/g in MS800, 3.35 mg/g in TS200 to 0.75 mg/g in TS800, and 2.50 mg/g in SS200 to 0.40 mg/g in SS800. As the temperature increases, the concentration of IP extracted is continuously increasing, the O-IP and Ca-IP content in the IP of MS, TS, and SS increased but the SL-IP, Al-IP, and Fe-IP content of MS and SS decreased, slightly differently the Al-IP content of TS increased with increasing temperature. The total of sequential fractions of the TP was 89.78–105.19% for MS, 95.54–108.80% for TS, and 90.61–102.67% for SS. The P recovery expressively decreased with heating temperature, thus demonstrating less available P speciations at high temperatures. Our results obviously indicated a model of P transplantation during pyrolysis treatment, where pyrolysis technique expressively increased O-IP and Ca-IP fractions at the consumption of reduced proportion of SL-IP, Al-IP, and Fe-IP. A similar model was reported in a previous study [23].

Table 3. P-fractionation concentrations and recovery in sludges and their biochar (mg g^{-1}).

Biochar	SL-IP	Al-IP	Fe-IP	O-IP	Ca-IP	OP	Total	Recovery
MS	1.78	2.03	1.83	0.48	0.08	6.96	12.5	105.19
MS200	1.41	2.15	2.18	0.65	0.18	5.88	13.86	89.78
MS350	0.24	0.50	1.18	2.04	8.60	7.98	19.89	103.28
MS500	0.13	0.50	1.27	2.39	10.92	9.84	24.46	102.41
MS650	0.03	0.15	1.04	1.92	17.80	1.98	21.93	104.52
MS800	0.01	0.17	1.58	1.03	19.68	0.61	22.72	101.54
TS	0.05	3.25	12.79	0.82	0.33	3.35	19.64	104.80
TS200	0.03	3.84	13.44	0.90	0.38	3.72	21.90	101.87
TS350	0.03	5.29	9.01	0.91	5.75	2.32	23.91	97.49
TS500	0.03	4.70	8.27	1.30	9.18	2.18	25.24	101.68
TS650	0.05	4.17	6.87	1.33	8.04	1.34	22.14	98.43
TS800	0.05	3.67	5.80	1.38	9.89	0.75	22.54	95.54
SS	0.31	1.43	4.29	0.37	0.09	2.50	9.70	92.67
SS200	0.51	1.89	4.46	0.54	0.18	2.40	11.01	90.61
SS350	0.05	0.79	2.55	1.12	10.73	2.27	17.07	102.67
SS500	0.04	0.73	2.36	1.89	12.96	1.65	19.56	100.32
SS650	0.01	0.06	2.47	2.09	12.80	1.28	18.66	100.28
SS800	0.01	0.08	2.20	1.22	13.77	0.40	18.15	97.33

Table 4 shows the rate of different speciation of phosphorus in sludges (MS, TS, and SS) and biochars pyrolyzed by sludges (MS, TS, and SS) in the temperature range of 200–800 °C. Phosphorus speciation in MS, TS, SS, and corresponding biochars from different temperatures are revealed in Figure 1. Among the three raw sludges, the organic phosphorus (OP) content in MS is the highest, and the organic phosphorus content in TS is the lowest. It is showed that MS has a higher

amount of OP than TS and SS, as a result of the biological removal of P during sewage disposal [42]. When the pyrolysis temperature rises to 650 °C, the OP content in MS is greatly reduced. When the pyrolysis temperature rises to 800°C, the OP content in all sludge is reduced to a minimum.

Table 4. The rate of P-fractionation in sludge and biochars (%).

Biochar	SL-IP	Al-IP	Fe-IP	O-IP	Ca-IP	OP
MS	12.71	14.52	13.11	3.41	0.58	55.67
MS200	12.33	18.84	19.11	5.74	1.60	42.38
MS350	1.16	2.37	5.62	9.74	41.00	40.11
MS500	0.51	1.97	4.99	9.38	42.91	40.23
MS650	0.13	0.66	4.51	8.35	77.31	9.04
MS800	0.04	0.74	6.83	4.44	85.27	2.68
TS	0.24	15.65	61.53	3.94	1.58	17.05
TS200	0.15	17.14	60.02	4.03	1.70	16.96
TS350	0.12	22.76	38.76	3.90	24.75	9.71
TS500	0.11	18.28	32.19	5.05	35.73	8.65
TS650	0.23	19.14	31.53	6.11	36.91	6.08
TS800	0.22	17.06	26.96	6.44	45.98	3.35
SS	3.59	16.32	49.08	4.18	1.00	25.83
SS200	5.22	19.49	46.04	5.58	1.88	21.80
SS350	0.31	4.51	14.52	6.36	61.00	13.30
SS500	0.19	3.71	12.04	9.61	66.02	8.42
SS650	0.05	0.33	13.20	11.18	68.39	6.86
SS800	0.03	0.43	12.46	6.93	77.98	2.18

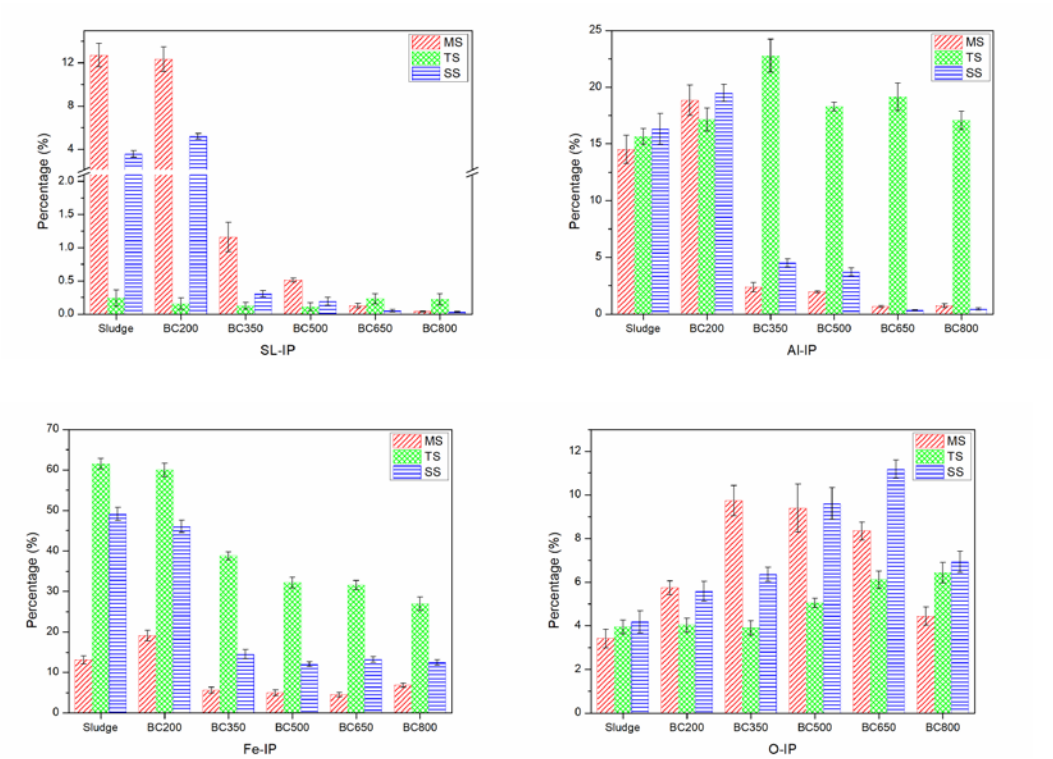

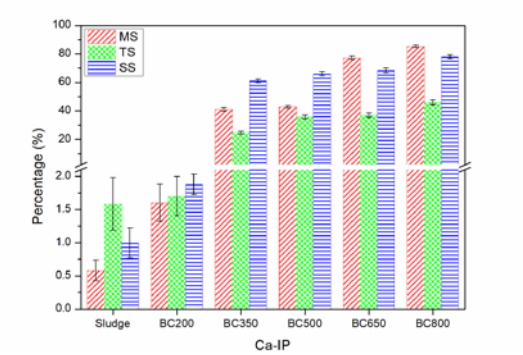

Figure 1. Percentages of phosphorus speciation in material and biochars.

OP accounted for about 55.67% of raw MS. After pyrolysis, OP proportion decreased to 2.68% at 800 °C. Raw TS contained 17.05% of OP, and when the pyrolysis temperature was elevated from 200 °C to 800 °C, OP content of TS decreased from 16.96% to 3.47%. OP concentration in biochar decreased gradually with heating temperature. OP of SS through slow pyrolysis at temperatures ranging from 250 °C to 800 °C and observed similar trends. After pyrolysis, TP concentration in biochar increased gradually with heating temperature. IP proportion in TP was enhanced while OP share was decreased. The decrease in the proportion of organic phosphorus may be due to the decomposition of organic matter during the pyrolysis process, resulting in the release of microbial intracellular phosphorus, which further reacts with the metal ions (Fe^{2+}, Al^{3+}) in the sludge at high temperatures, leading to the formation of more types of IP [43].

Raw MS contained 12.71% of SL-IP. After pyrolysis, SL-IP content in biochar decreased gradually with heating temperature. Pyrolysis of TS at ≥ 200 °C reduced SL-IP from 0.24% to 0.10%. Thermal treatments of TS at 650–800 °C SL-IP increased from 0.10% to 0.22%. Conversion of SS into biochar through slow pyrolysis at ≥ 350 °C decreased SL-IP from 3.59% to below 0.03%. The proportion of SL-IP expressively decreased at 350 °C and was unchanged at higher temperatures. The SL-IP values were 12.71%, 0.24%, and 3.59% for raw MS, raw TS, and raw SS, respectively. The content of SL-IP of TS is much lower compared to MS and SS, and this may be due to the different of the removal of P and in the subsequent processing of sewage sludge [44]. These values were expressively reduced confronted with 0.13% in MS650, 0.23% in TS650, and 0.05% in SS650. These results are similar to those gained in a previous work where pyrolysis at 300 °C expressively reduced the s SL-IP fraction of > 25% in wheat straw, maize straw, and peanut husk to <11% in their biochars [38]. Cantrell et al. [39] also indicated that the expressively reduced SL-IP in manure biochar was due to pyrolysis temperature. In environmental studies, SL-IP is a prominent indicator of the short-term P loss possible in biosolids, which results in eutrophication of aquatic ecosystem [45].

As observed, Al-IP accounted for 14.52% of IP in raw MS, with increasing pyrolysis temperature Al-IP proportion increased to 18.84% at 200 °C and then decreased with rising temperature. The amounts of Al-IP of TS were initially increased at 200 °C–350 °C and then decreased to 18.28% at 500 °C. However, when the pyrolysis temperature was increased to 650 °C Al-IP content of TS increased to 19.14%, and then decreased to 17.06% at 800 °C. Raw SS has Al-IP content about 16.32%, after pyrolysis, AI-IP proportion increased to 19.49% at 200 °C and then decreased with rising temperature. Among the three raw sludges, the content of Al-IP is similar, but

after pyrolysis, the content of Al-IP in TS does not decrease much compared with MS and SS. This may be because the TS was gathered from a rural sewage disposal plant, the large amount of clay minerals mixed into the TS, and the clay minerals have a higher content of Al.

Fe-IP accounted for 13.11% of IP in raw MS, with increasing pyrolysis temperature Fe-IP proportion increased to 19.11% at 200 °C and then decreased with rising temperature but Fe-IP proportion increased from 4.51% to 6.82% at 650–800 °C. Fe-IP accounted for 61.53% of IP in raw TS, which is the major species of IP in raw TS. When the pyrolysis temperature increases from 200 °C to 800 °C, Fe-IP content of TS decreased from 60.02% to 26.96%. Raw SS has Fe-IP content about 49.08%, when the pyrolysis temperature increases from 200 °C to 500 °C Fe-IP content of SS decreased from 46.04% to 12.04%, but Fe-IP proportion increased to 13.20% at 650 °C and then decreased with rising temperature.

Raw MS has O-IP content of about 3.41%. The amounts of O-IP of MS were initially increased at 200–350 °C and then decreased with rising temperature. Raw TS has O-IP content about 3.94%, after pyrolysis, O-IP proportion increased to 4.03% at 200 °C, but when the temperature increases from 200 °C to 350 °C, O-IP content decreased to 3.9% and then increased with rising temperature. And raw SS has O-IP content about 4.18%. When the pyrolysis temperature increased from 200 °C to 650 °C, O-IP content of SS increased from 5.58% to 11.18%, but O-IP proportion decreased to 6.93% at 800 °C.

All biochars prepared from sludge revealed expressively increased Ca-IP content with increasing pyrolysis temperature where Ca-IP increased from 0.58% in raw MS to 85.27% in MS800, 1.58% in raw TS to 45.98% in TS800, and 1.00% in raw SS to 77.98% in SS800. Compared with MS and SS, the formation of Ca-IP in TS is less. This may be due to the content of organophosphorus in TS was lower than that in MS and SS. The conversion of organophosphorus during pyrolysis is the main factor for the formation of Ca-IP [28]. Second, it could be due to the low conversion of Al-IP and Fe-IP of TS during pyrolysis, as Al-IP and Fe-IP were found to be stable at high temperatures [46,47]. Notably, Ca-IP was expressively increased in the sludge biochar than in the feedstock. At lower pyrolysis temperature, carboxyl and carbonyl groups would be reacting with Ca, restraining massive formation of insoluble P forms. These groups, however, evaporate at high temperatures. Therefore, when the pyrolysis temperature was 500 °C or higher, the more aromatic structure of the biochars would not inhibit the constitution of Ca-IP compounds [48].

The influence of temperature during the pyrolysis is important for the mineral structure of the sludges. XRD measurement showed the presence of many crystallized minerals in sludge and their biochar. The acquired XRD curves of the sludge and their biochar and the peaks of the minerals appeared in the samples have been signaled with number symbols in Figure 2 and Table 5. We found that the aluminum ion (Al^{3+}) combined with orthophosphate ions (PO_4^{3-}) in raw MS, TS, and SS to constitute $AlPO_4$, which appeared in the form of non-apatite inorganic phosphorus. When the pyrolysis temperature was 200–500 °C, some apatite containing hydroxyl group appeared, which was more easily absorbed and utilized by plants. When the temperature reached 650–800 °C, various phosphorus speciations in biochars were gradually converted to $Ca_2Pb_8(PO_4)_6(OH)_2$, $Ca_{5.5}Pb_{4.5}(PO_4)_6(OH)_2$, $Ca_9HPO_4(PO_4)_5OH$), and other more stable orthophosphates [49]. The crystal phases of $AlPO_4$, $Fe_4(PO_4)_3(OH)_3$, $Fe_3(PO_4)_2(OH)_2$, $Fe_3(PO_4)_2{\cdot}H_2O$, $Ca_2P_2O_7$, CaP_2O_6, and $Ca_{5.5}Pb_{4.5}(PO_4)_6(OH)_2$ were found in raw MS. Besides, other new crystal phases such as

$Fe_5(PO_4)_3(OH)_5$, $FePO_4{\cdot}2H_2O$, $Fe_4(PO_4)_3(OH)_3{\cdot}5H_2O$, $Fe_2PO_4(OH)$, $Ca_4P_6O_{19}$, $Ca_3(PO_4)_2$, $Ca_2Pb_8(PO_4)_6(OH)_2$, and $Ca_9HPO_4(PO_4)_5OH$ were found in MS200, MS350, MS500, MS650, and MS800 and did not appear in MS. In particular, the crystal phase of $Ca_9HPO_4(PO_4)_5OH$ only existed in MS650. The crystal phases of $AlPO_4$, $Fe_4(PO_4)_3(OH)_3$, $Fe_3(PO_4)_2(OH)_2$, $Fe_5(PO_4)_3(OH)_5$, $Fe_4(PO_4)_3(OH)_3{\cdot}5H_2O$, $Fe_3(PO_4)_2{\cdot}H_2O$, $Fe_2PO_4(OH)$, and $Ca_2P_2O_7$ were found in raw TS. New peaks such as $FePO_4{\cdot}2H_2O$, $Ca_4P_6O_{19}$, and $Ca_3(PO_4)_2$ occurred in the XRD curves produced from the TS200, TS350, TS500, and TS650. It is worth noting that a lot of new peaks such as ($Ca_2Pb_8(PO_4)_6(OH)_2$, $Ca_{5.5}Pb_{4.5}(PO_4)_6(OH)_2$, and $Ca_9HPO_4(PO_4)_5OH$) appeared in the XRD curves of TS800. The XRD curves of raw SS almost coincided with raw MS, and an increase (200–650 °C) and decrease (650–800 °C) of the species of crystal phases can be found in their biochar. The results are in accordance with a previous study [31]. Similarly, the crystal phases of $Ca_2Pb_8(PO_4)_6(OH)_2$ and $Ca_9HPO_4(PO_4)_5OH$) appeared in the XRD curves of SS650. It is worth mentioning that the P, which is adsorbed in the lattice of the minerals, is steadier than that adsorbed on raw sludges. Those P-containing minerals are difficult to release and therefore difficult to use in the short term [23]. This could be the real reason for the stabilization of P convert to the H_2SO_4-extract (Ca-IP) at high temperatures (e.g., 800 °C). Lipscombite ($Fe_3(PO_4)_2(OH)_2$) was detected in all the XRD curves (Figure 2). In addition, the peak position was confronted with patterns of these minerals appeared in other works [50,51]. Lipscombite is normally formed P-minerals during sewage disposal and P-removal with Fe-salts. These mineral phases are the base for the probe into P conversion during pyrolysis. The XRD analysis fingered that in addition to the compounds of orthophosphate, other compounds of pyrophosphate could not be spotted, though these compounds accounted for a sizeable proportion of the total phosphorus in the biochars, which may be caused by the combinations between P and biochar in which P could be adsorbed on Al, Fe, or Ca, same as in soil [26]. The conclusions from the XRD curves of the MS and SS are compliance with the outcomes of the transplantations of P from Fe-IP and Al-IP to Ca-IP at the stated temperature ranges. Therefore, biochars disposed at low temperature (0–200 °C) revealed tiny differences in their XRD curves, proving that the types of P compounds in the biochars disposed at low temperatures are similar hence revealing comparable quantities of Fe-IP, Al-IP, and Ca-IP in these biochars. Nevertheless, biochars disposed at high temperature (350−800 °C) formed a new type of P-containing mineral, a considerable proportion of which would be stabilized in the minerals, resulting in a noteworthy increase of Ca-IP of these biochars.

Table 5. The crystal phases of phosphorus at different pyrolysis temperatures.

MS	MS200	MS350	MS500	MS650	MS800
1.$AlPO_4$	1.$AlPO_4$	1.$AlPO_4$	1.$AlPO_4$	1.$AlPO_4$	1.$AlPO_4$
2.$Fe_4(PO_4)_3(OH)_3$	2.$Fe_4(PO_4)_3(OH)_3$	2.$Fe_4(PO_4)_3(OH)_3$	2.$Fe_4(PO_4)_3(OH)_3$	2.$Fe_4(PO_4)_3(OH)_3$	2.$Fe_4(PO_4)_3(OH)_3$
3.$Fe_3(PO_4)_2(OH)_2$	3.$Fe_3(PO_4)_2(OH)_2$	3.$Fe_3(PO_4)_2(OH)_2$	3.$Fe_3(PO_4)_2(OH)_2$	3.$Fe_3(PO_4)_2(OH)_2$	3.$Fe_3(PO_4)_2(OH)_2$
7.$Fe_3(PO_4)_2{\cdot}H_2O$	4. $Fe_5(PO_4)_3(OH)_5$	4. $Fe_5(PO_4)_3(OH)_5$	4. $Fe_5(PO_4)_3(OH)_5$	4. $Fe_5(PO_4)_3(OH)_5$	4. $Fe_5(PO_4)_3(OH)_5$
9.$Ca_2P_2O_7$	6. $Fe_4(PO_4)_3(OH)_3{\cdot}5H_2O$	6. $Fe_4(PO_4)_3(OH)_3{\cdot}5H_2O$	5. $FePO_4{\cdot}2H_2O$	7.$Fe_3(PO_4)_2{\cdot}H_2O$	7.$Fe_3(PO_4)_2{\cdot}H_2O$
10.CaP_2O_6	7.$Fe_3(PO_4)_2{\cdot}H_2O$	7.$Fe_3(PO_4)_2{\cdot}H_2O$	6. $Fe_4(PO_4)_3(OH)_3{\cdot}5H_2O$	9.$Ca_2P_2O_7$	9.$Ca_2P_2O_7$
14.$Ca_{5.5}Pb_{4.5}(PO_4)_6(OH)_2$	9.$Ca_2P_2O_7$	9.$Ca_2P_2O_7$	7.$Fe_3(PO_4)_2{\cdot}H_2O$	10.CaP_2O_6	11. $Ca_4P_6O_{19}$
	14.$Ca_{5.5}Pb_{4.5}(PO_4)_6(OH)_2$	12.$Ca_3(PO_4)_2$	9.$Ca_2P_2O_7$	12.$Ca_3(PO_4)_2$	12.$Ca_3(PO_4)_2$
		14.$Ca_{5.5}Pb_{4.5}(PO_4)_6(OH)_2$	10.CaP_2O_6	13.$Ca_2Pb_8(PO_4)_6(OH)_2$	13.$Ca_2Pb_8(PO_4)_6(OH)_2$
			11. $Ca_4P_6O_{19}$	14.$Ca_{5.5}Pb_{4.5}(PO_4)_6(OH)_2$	
			12.$Ca_3(PO_4)_2$	15. $Ca_9HPO_4(PO_4)_5OH$	
			14.$Ca_{5.5}Pb_{4.5}(PO_4)_6(OH)_2$		
TS	TS200	TS350	TS500	TS650	TS800
1.$AlPO_4$	1.$AlPO_4$	1.$AlPO_4$	1.$AlPO_4$	1.$AlPO_4$	1.$AlPO_4$
2.$Fe_4(PO_4)_3(OH)_3$	2.$Fe_4(PO_4)_3(OH)_3$	2.$Fe_4(PO_4)_3(OH)_3$	2.$Fe_4(PO_4)_3(OH)_3$	2.$Fe_4(PO_4)_3(OH)_3$	2.$Fe_4(PO_4)_3(OH)_3$
3.$Fe_3(PO_4)_2(OH)_2$	3.$Fe_3(PO_4)_2(OH)_2$	3.$Fe_3(PO_4)_2(OH)_2$	3.$Fe_3(PO_4)_2(OH)_2$	3.$Fe_3(PO_4)_2(OH)_2$	3.$Fe_3(PO_4)_2(OH)_2$
4. $Fe_5(PO_4)_3(OH)_5$	4. $Fe_5(PO_4)_3(OH)_5$	6. $Fe_4(PO_4)_3(OH)_3{\cdot}_5H_2O$	4. $Fe_5(PO_4)_3(OH)_5$	4. $Fe_5(PO_4)_3(OH)_5$	4. $Fe_5(PO_4)_3(OH)_5$
6. $Fe_4(PO_4)_3(OH)_3{\cdot}5H_2O$	6. $Fe_4(PO_4)_3(OH)_3{\cdot}5H_2O$	7.$Fe_3(PO_4)_2{\cdot}H_2O$	5. $FePO_4{\cdot}2H_2O$	5. $FePO_4{\cdot}2H_2O$	5. $FePO_4{\cdot}2H_2O$
7.$Fe_3(PO_4)_2{\cdot}H_2O$	7.$Fe_3(PO_4)_2{\cdot}H_2O$	9.$Ca_2P_2O_7$	6. $Fe_4(PO_4)_3(OH)_3{\cdot}5H_2O$	6. $Fe_4(PO_4)_3(OH)_3{\cdot}5H_2O$	6. $Fe_4(PO_4)_3(OH)_3{\cdot}5H_2O$
8. $Fe_2PO_4(OH)$	9.$Ca_2P_2O_7$	12.$Ca_3(PO_4)_2$	7.$Fe_3(PO_4)_2{\cdot}H_2O$	7.$Fe_3(PO_4)_2{\cdot}H_2O$	7.$Fe_3(PO_4)_2{\cdot}H_2O$
9.$Ca_2P_2O_7$	11. $Ca_4P_6O_{19}$		8. $Fe_2PO_4(OH)$	8. $Fe_2PO_4(OH)$	8. $Fe_2PO_4(OH)$
	12.$Ca_3(PO_4)_2$		9.$Ca_2P_2O_7$	9.$Ca_2P_2O_7$	9.$Ca_2P_2O_7$
			12.$Ca_3(PO_4)_2$	12.$Ca_3(PO_4)_2$	10.CaP_2O_6
					11. $Ca_4P_6O_{19}$
					12.$Ca_3(PO_4)_2$
					13.$Ca_2Pb_8(PO_4)_6(OH)_2$
					14.$Ca_{5.5}Pb_{4.5}(PO_4)_6(OH)_2$
					15. $Ca_9HPO_4(PO_4)_5OH$
SS	SS200	SS350	SS500	SS650	SS800
1.$AlPO_4$	1.$AlPO_4$	1.$AlPO_4$	1.$AlPO_4$	1.$AlPO_4$	1.$AlPO_4$
2.$Fe_4(PO_4)_3(OH)_3$	2.$Fe_4(PO_4)_3(OH)_3$	2.$Fe_4(PO_4)_3(OH)_3$	2.$Fe_4(PO_4)_3(OH)_3$	2.$Fe_4(PO_4)_3(OH)_3$	2.$Fe_4(PO_4)_3(OH)_3$
3.$Fe_3(PO_4)_2(OH)_2$	3.$Fe_3(PO_4)_2(OH)_2$	3.$Fe_3(PO_4)_2(OH)_2$	3.$Fe_3(PO_4)_2(OH)_2$	3.$Fe_3(PO_4)_2(OH)_2$	3.$Fe_3(PO_4)_2(OH)_2$
4. $Fe_5(PO_4)_3(OH)_5$	4. $Fe_5(PO_4)_3(OH)_5$	4. $Fe_5(PO_4)_3(OH)_5$	4. $Fe_5(PO_4)_3(OH)_5$	4. $Fe_5(PO_4)_3(OH)_5$	4. $Fe_5(PO_4)_3(OH)_5$

Continued on next page

6. $Fe_4(PO_4)_3(OH)_3{\cdot}5H_2O$	6. $Fe_4(PO_4)_3(OH)_3{\cdot}5H_2O$	6. $Fe_4(PO_4)_3(OH)_3{\cdot}5H_2O$	6. $Fe_4(PO_4)_3(OH)_3{\cdot}5H_2O$	7.$Fe_3(PO_4)_2{\cdot}H_2O$	7.$Fe_3(PO_4)_2{\cdot}H_2O$
7.$Fe_3(PO_4)_2{\cdot}H_2O$	7.$Fe_3(PO_4)_2{\cdot}H_2O$	9.$Ca_2P_2O_7$	7.$Fe_3(PO_4)_2{\cdot}H_2O$	9.$Ca_2P_2O_7$	12.$Ca_3(PO_4)_2$
9.$Ca_2P_2O_7$	9.$Ca_2P_2O_7$	10.CaP_2O_6	9.$Ca_2P_2O_7$	10.CaP_2O_6	14.$Ca_{5.5}Pb_{4.5}(PO_4)_6(OH)_2$
10.CaP_2O_6		11. $Ca_4P_6O_{19}$	10.CaP_2O_6	11. $Ca_4P_6O_{19}$	
14.$Ca_{5.5}Pb_{4.5}(PO_4)_6(OH)_2$			12.$Ca_3(PO_4)_2$	12.$Ca_3(PO_4)_2$	
			14.$Ca_{5.5}Pb_{4.5}(PO_4)_6(OH)_2$	13.$Ca_2Pb_8(PO_4)_6(OH)_2$	
			15. $Ca_9HPO_4(PO_4)_5OH$	15. $Ca_9HPO_4(PO_4)_5OH$	

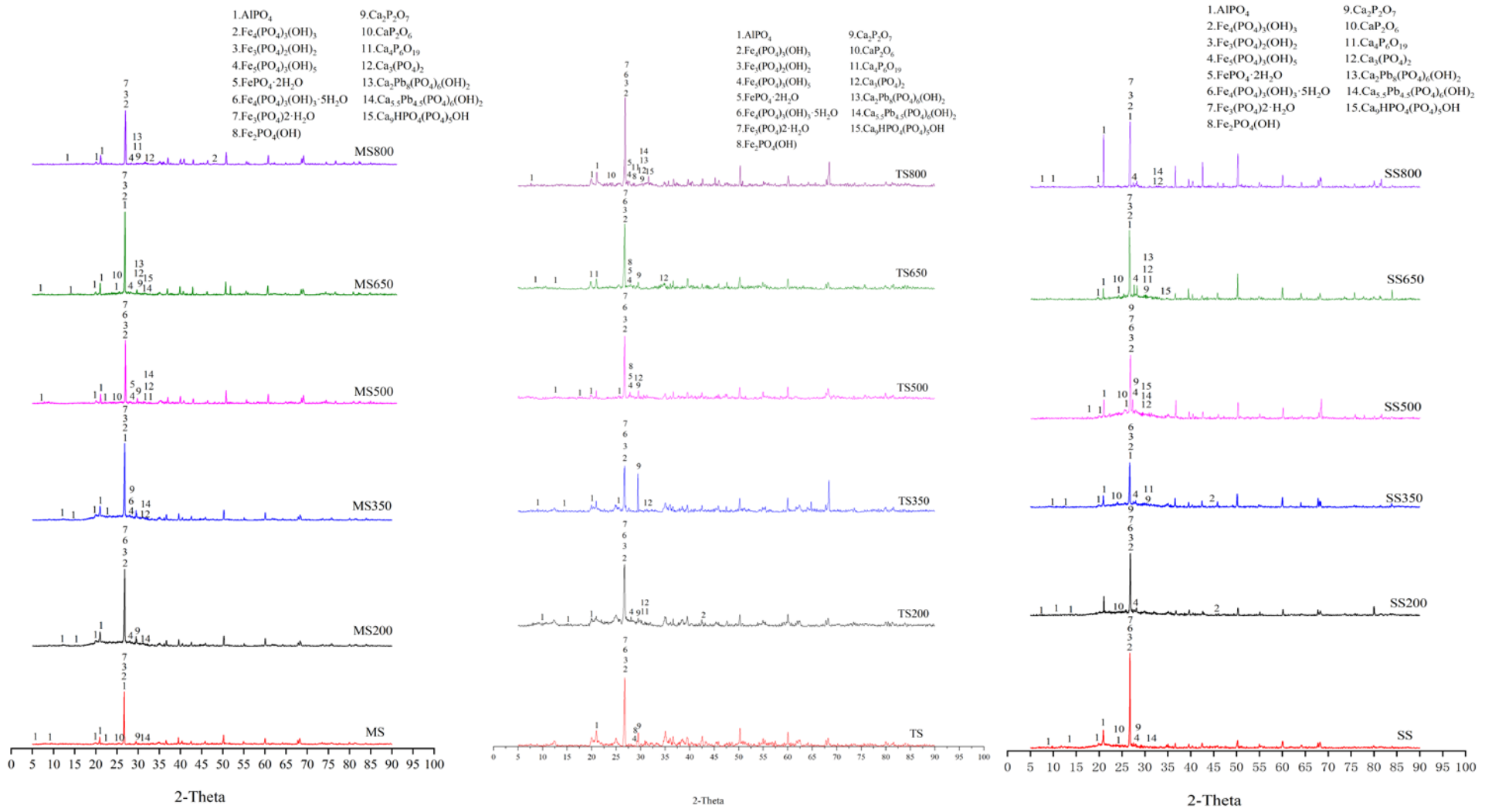

Figure 2. X-ray diffraction diagrams of MS, TS, SS, and their biochars.

3.3. Changes of Olsen-P before and after pyrolysis

The contents of Olsen-p of the MS, TS and SS and their biochar were shown in Table 6. Of the three raw sludges, MS has the highest Olsen-p content, while TS has the lowest, as the Olsen-p content decreases with the decrease of pH due to the acidification treatment in the wastewater treatment project, which has also been reported in other study [52]. When the pyrolysis temperature reaches 200 ℃, the content of Olsen-p of all samples increased. When the pyrolysis temperature continues to rise, the content of Olsen-p decreased. The rate of Olsen-p in three different sludges and their biochar were shown in Table 7. It revealed that the rate of Olsen-p in biochar decreased as temperature increased. Thermal process reduce the fraction of mobile P phases (Olsen-P) and transplants more P into less mobile phases (O-IP and Ca-IP) [41]. Therefore, with the increase of temperature, there was an distinct tendency for P to move towards less available speciations. Our results are consistent with previous works, the reduction of Olsen P was watched during the pyrolysis of sewage sludges [53], plant biomass [38], and livestock manures [54]. For instance, Christel et al. [55] determined phosphorus availability in solid fractions of pig manure biochar using diffusive gradients in thinfilm technology. The results showed that the availability of phosphorus decreases greatly with the increase of temperature. The reduced Olsen P in biochar may be because of the formation of stable aromatic or crystalline insoluble compounds during pyrolysis process [56,57].

Table 6. The concentration of Olsen-P in sludge and biochars (mg g^{-1}).

Samples	Sludge	Biochar (°C)				
		200	350	500	650	800
MS	1.48	1.89	0.32	0.24	0.25	0.32
TS	0.46	1.18	0.70	0.52	0.43	0.37
SS	0.61	0.65	0.35	0.13	0.26	0.13

Table 7. The rate of Olsen-P in sludge and biochars.

Samples	Sludge	Biochar (°C)				
		200	350	500	650	800
MS	11.86	13.65	1.61	0.98	1.16	1.43
TS	2.36	5.39	2.92	2.06	1.94	1.64
SS	6.299	5.87	2.05	0.66	1.40	0.74

4. Conclusions

Sludge and its derived biochar are widely used in soil amendments and construction materials. Mastering the speciation of phosphorus is of great significance for further understanding of the potential impact of phosphorus in sludge and its derived biochar on the environment. The results of this study showed the phosphorus speciation changes in biochar after pyrolysis of sludge was hinge on both sewage disposal techniques and raw material composition. XRD analysis and sequential extraction revealed the immobilization of P after pyrolysis, because of the forming of relatively stable Ca-associated P speciation as same as underlying physical constraints. The degradation of

organic phosphates and the crystallization of calcium phosphate minerals are detected during the pyrolysis process, and were highly dependent on the pyrolysis temperature. As a result, phosphorus is better immobilized when the pyrolysis temperature is higher and extracted primarily by H_2SO_4. Results from the study afforded deeper perceptions into the thermochemical processes occurred during the pyrolysis of sludges, as well as guidance for P conversion and transplantation from these sludges.

Use of AI tools declaration

The authors declare they have not used Artificial Intelligence (AI) tools in the creation of this article.

Acknowledgements

This work was financially supported by the National Natural Science Foundation of China (42107435), Key Research and Development Programs of Hunan (2020NK2011, 2021NK2012), Key Project Science Foundation of Hunan Education Department, China (21A0143, 21A0132).

Conflict of interest

The authors declare no conflict of interest.

References

1. Wu Q, Zou D, Zheng X, et al. (2022) Effects of antibiotics on anaerobic digestion of sewage sludge: Performance of anaerobic digestion and structure of the microbial community. *Sci Total Environ* 845: 157384. https://doi.org/10.1016/j.scitotenv.2022.157384
2. Keeffe AO, Brooks E, Dunkel C, et al. (2023) Soil moisture routing modeling of targeted biochar amendment in undulating topographies : an analysis of biochar ' s effects on streamflow. *AIMS Environ Sci* 10: 529–546. https://doi.org/10.3934/environsci.2023030
3. Guo Y, Guo Y, Gong H, et al. (2021) Variations of heavy metals, nutrients, POPs and particle size distribution during 'sludge anaerobic digestion-solar drying-land utilization process': Case study in China. *Sci Total Environ* 801: 149609. https://doi.org/10.1016/j.scitotenv.2021.149609
4. Feng H, Zheng M, Dong H, et al. (2015) Three-dimensional honeycomb-like hierarchically structured carbon for high-performance supercapacitors derived from high-ash-content sewage sludge. *J Mater Chem A* 3: 15225–15234. https://doi.org/10.1039/C5TA03217B
5. Yuan S-J, Dai X-H (2015) Heteroatom-doped porous carbon derived from "all-in-one" precursor sewage sludge for electrochemical energy storage. *RSC Adv* 5: 45827–45835. https://doi.org/10.1039/C5RA07178J
6. Zhang J, Lü F, Zhang H, et al. (2015) Multiscale visualization of the structural and characteristic changes of sewage sludge biochar oriented towards potential agronomic and environmental implication. *Sci Rep* 5: 9406. https://doi.org/10.1038/srep09406

7. Yue Y, Cui L, Lin Q, et al. (2017) Efficiency of sewage sludge biochar in improving urban soil properties and promoting grass growth. *Chemosphere* 173: 551–556. https://doi.org/10.1016/j.chemosphere.2017.01.096
8. Fang S, Tsang DCW, Zhou F, et al. (2016) Stabilization of cationic and anionic metal species in contaminated soils using sludge-derived biochar. *Chemosphere* 149: 263–271. https://doi.org/10.1016/j.chemosphere.2016.01.060
9. Rathnayake N, Patel S, Halder P, et al. (2022) Co-pyrolysis of biosolids with alum sludge: Effect of temperature and mixing ratio on product properties. *J Anal Appl Pyrolysis* 163: 105488. ttps://doi.org/10.1016/j.jaap.2022.105488
10. Zielińska A, Oleszczuk P (2016) Attenuation of phenanthrene and pyrene adsorption by sewage sludge-derived biochar in biochar-amended soils. *Environ Sci Pollut Res* 23: 21822–21832. tps://doi.org/10.1007/s11356-016-7382-x
11. Zielińska A, Oleszczuk P (2016) Bioavailability and bioaccessibility of polycyclic aromatic hydrocarbons (PAHs) in historically contaminated soils after lab incubation with sewage sludge-derived biochars. *Chemosphere*. https://doi.org/10.1016/j.chemosphere.2016.08.072
12. Mayer BK, Baker LA, Boyer TH, et al. (2016) Total Value of Phosphorus Recovery. *Environ Sci Technol* 50: 6606–6620. https://doi.org/10.1021/acs.est.6b01239
13. Hossain MK, Strezov Vladimir V, Chan KY, et al. (2011) Influence of pyrolysis temperature on production and nutrient properties of wastewater sludge biochar. *J Environ Manage* 92: 223–228. https://doi.org/10.1016/j.jenvman.2010.09.008
14. Khan S, Chao C, Waqas M, et al. (2013) Sewage sludge biochar influence upon rice (Oryza sativa L) yield, metal bioaccumulation and greenhouse gas emissions from acidic paddy soil. *Environ Sci Technol* 47: 8624–8632. https://doi.org/10.1021/es400554x
15. Moško J, Pohořelý M, Skoblia S, et al. (2021) Structural and chemical changes of sludge derived pyrolysis char prepared under different process temperatures. *J Anal Appl Pyrolysis* 156: 105085. https://doi.org/10.1016/j.jaap.2021.105085
16. Liu Q-S, Tian T (2021) Co-pyrolysis of iron-rich sewage sludge and potassium phosphate to prepare biochars: P fractionation and alleviated occlusion. *J Anal Appl Pyrolysis* 159: 105285. https://doi.org/10.1016/j.jaap.2021.105285
17. Tang S, Liang J, Xu X, et al. (2023) Targeting phosphorus transformation to hydroxyapatite through sewage sludge pyrolysis boosted by quicklime toward phosphorus fertilizer alternative with toxic metals compromised. *Renew Sustain Energy Rev*. https://doi.org/10.2139/ssrn.4416963
18. Wisawapipat W, Charoensri K, Runglerttrakoolchai J (2017) Solid-phase speciation and solubility of phosphorus in an acid sulfate paddy soil during soil reduction and reoxidation as affected by oil palm ash and biochar. *J Agric Food Chem* 65: 704–710. https://doi.org/10.1021/acs.jafc.6b03925
19. Huang R, Tang Y (2015) Speciation Dynamics of Phosphorus during (Hydro)Thermal Treatments of Sewage Sludge. *ACS Publ* 49: 14466–14474. https://doi.org/10.1021/acs.est.5b04140

20. Chakraborty D, Nair VD, Harris WG (2012) Compositional differences between alaquods and paleudults affecting phosphorus sorption-desorption behavior. *Soil Sci* 177: 188–197. https://doi.org/10.1097/SS.0b013e31824329ca
21. Pant H, Reddy K. (2003) Potential internal loading of phosphorus in a wetland constructed in agricultural land. *Water Res* 37: 965–972. https://doi.org/10.1016/S0043-1354(02)00474-8
22. Qin B, Zhou J, Elser JJ, et al. (2020) Water Depth Underpins the Relative Roles and Fates of Nitrogen and Phosphorus in Lakes. *Environ Sci Technol* 54: 3191–3198. https://doi.org/10.1021/acs.est.9b05858
23. Qian TT, Jiang H (2014) Migration of phosphorus in sewage sludge during different thermal treatment processes. *ACS Sustain Chem Eng* 2: 1411–1419. https://doi.org/10.1021/sc400476j
24. Hamdan R, El-Rifai HM, Cheesman AW, et al. (2012) Linking Phosphorus Sequestration to Carbon Humification in Wetland Soils by 31 P and 13 C NMR Spectroscopy. *Environ Sci Technol* 46: 4775–4782. https://doi.org/10.1021/es204072k
25. McDowell RW, Condron LM, Mahieu N, et al. (2002) Analysis of Potentially Mobile Phosphorus in Arable Soils Using Solid State Nuclear Magnetic Resonance. *J Environ Qual* 31: 450–456. https://doi.org/10.2134/jeq2002.4500
26. Sharpley AN, McDowell RW, Kleinman PJA (2004) Amounts, Forms, and Solubility of Phosphorus in Soils Receiving Manure. *Soil Sci Soc Am J* 68: 2048–2057. https://doi.org/10.2136/sssaj2004.2048
27. Chang SC, Jackson ML (1957) Fractionation of soil phosphorus. *Soil Sci*. https://doi.org/10.1097/00010694-195708000-00005
28. Kleemann R, Chenoweth J, Clift R, et al. (2017) Comparison of phosphorus recovery from incinerated sewage sludge ash (ISSA) and pyrolysed sewage sludge char (PSSC). *Waste Manag*. ttps://doi.org/10.1016/j.wasman.2016.10.055
29. Fang Z, Liu F, Li Y, et al. (2021) Influence of microwave-assisted pyrolysis parameters and additives on phosphorus speciation and transformation in phosphorus-enriched biochar derived from municipal sewage sludge. *J Clean Prod* 287. https://doi.org/10.1016/j.jclepro.2020.125550
30. Shao J, Yuan X, Leng L, et al. (2015) The comparison of the migration and transformation behavior of heavy metals during pyrolysis and liquefaction of municipal sewage sludge, paper mill sludge, and slaughterhouse sludge. *Bioresour Technol* 198: 16–22. https://doi.org/10.1016/j.biortech.2015.08.147
31. Zeng X, Xiao Z, Zhang G, et al. (2018) Speciation and bioavailability of heavy metals in pyrolytic biochar of swine and goat manures, Elsevier B.V. https://doi.org/10.1016/j.jaap.2018.03.012
32. Backnäs S, Laine-Kaulio H, Kløve B (2012) Phosphorus forms and related soil chemistry in preferential flowpaths and the soil matrix of a forested podzolic till soil profile. *Geoderma* 189–190: 50–64. https://doi.org/10.1016/j.geoderma.2012.04.016
33. Anal C (1962) Amodified single solution method for the determination of phosphate in natural waters. *Anal Chim Acta* 8: 31–36. https://doi.org/10.1016/S0003-2670(00)88444-5
34. Fife C V. (1959) An evaluation of ammonium fluoride as a selective extractant for aluminum-bound soil phosphate: II. Preliminary studies on soils. *Soil Sci*. https://doi.org/10.1097/00010694-195902000-00004

35. Xiao Z, Yuan X, Li H, et al. (2015) Chemical speciation, mobility and phyto-accessibility of heavy metals in fly ash and slag from combustion of pelletized municipal sewage sludge. *Sci Total Environ* 536: 774–783. https://doi.org/10.1016/j.scitotenv.2015.07.126
36. Romero-Freire A, Martin Peinado FJ, van Gestel CAM (2015) Effect of soil properties on the toxicity of Pb: Assessment of the appropriateness of guideline values. *J Hazard Mater* 289: 46–53. https://doi.org/10.1016/j.jhazmat.2015.02.034
37. Fang Z, Liu F, Li Y, et al. (2021) Influence of microwave-assisted pyrolysis parameters and additives on phosphorus speciation and transformation in phosphorus-enriched biochar derived from municipal sewage sludge. *J Clean Prod* 287: 125550. https://doi.org/10.1016/j.jclepro.2020.125550
38. Xu G, Zhang Y, Shao H, et al. (2016) Pyrolysis temperature affects phosphorus transformation in biochar: Chemical fractionation and 31P NMR analysis. *Sci Total Environ* 569–570: 65–72. https://doi.org/10.1016/j.scitotenv.2016.06.081
39. Cantrell KB, Hunt PG, Uchimiya M, et al. (2012) Impact of pyrolysis temperature and manure source on physicochemical characteristics of biochar. *Bioresour Technol* 107: 419–428. https://doi.org/10.1016/j.biortech.2011.11.084
40. Wang T, Camps-Arbestain M, Hedley M, et al. (2012) Predicting phosphorus bioavailability from high-ash biochars. *Plant Soil* 357: 173–187. https://doi.org/10.1007/s11104-012-1131-9
41. Huang R, Fang C, Lu X, et al. (2017) Transformation of Phosphorus during (Hydro)thermal Treatments of Solid Biowastes: Reaction Mechanisms and Implications for P Reclamation and Recycling. *Environ Sci Technol* 51: 10284–10298. https://doi.org/10.1021/acs.est.7b02011
42. Kuroda A, Takiguchi N, Gotanda T, et al. (2002) A simple method to release polyphosphate from activated sludgefor phosphorus reuse and recycling. *Biotechnol Bioeng*. https://doi.org/10.1002/bit.10205
43. Liu Q, Fang Z, Liu Y, et al. (2019) Phosphorus speciation and bioavailability of sewage sludge derived biochar amended with CaO. *Waste Manag* 87: 71–77. https://doi.org/10.1016/j.wasman.2019.01.045
44. Steckenmesser D, Vogel C, Adam C, et al. (2017) Effect of various types of thermochemical processing of sewage sludges on phosphorus speciation, solubility, and fertilization performance. *Waste Manag* 62: 194–203. https://doi.org/10.1016/j.wasman.2017.02.019
45. Li R, Wang JJ, Zhou B, et al. (2016) Enhancing phosphate adsorption by Mg/Al layered double hydroxide functionalized biochar with different Mg/Al ratios. *Sci Total Environ* 559: 121–129. https://doi.org/10.1016/j.scitotenv.2016.03.151
46. Zhang Q, Liu H, Li W, et al. (2012) Behavior of phosphorus during co-gasification of sewage sludge and coal, *Energy and Fuels*. https://doi.org/10.1021/ef300006d
47. Nanzer S, Oberson A, Huthwelker T, et al. (2014) The Molecular Environment of Phosphorus in Sewage Sludge Ash: Implications for Bioavailability. *J Environ Qual*. https://doi.org/10.2134/jeq2013.05.0202
48. Adhikari S, Gascó G, Méndez A, et al. (2019) Science of the Total Environment In fl uence of pyrolysis parameters on phosphorus fractions of biosolids derived biochar. *Sci Total Environ* 695: 133846. https://doi.org/10.1016/j.scitotenv.2019.133846

49. Li J, Li Y, Liu F, et al. (2023) Pyrolysis of sewage sludge to biochar: Transformation mechanism of phosphorus. *J Anal Appl Pyrolysis* 173: 106065. https://doi.org/10.1016/j.jaap.2023.106065
50. Frossard E, Bauer JP, Lothe F (1997) Evidence of vivianite in FeSO4 - Flocculated sludges. *Water Res*. https://doi.org/10.1016/S0043-1354(97)00101-2
51. Huang X-L, Shenker M (2004) Water-Soluble and Solid-State Speciation of Phosphorus in Stabilized Sewage Sludge. *J Environ Qual*. https://doi.org/10.2134/jeq2004.1895
52. Li S, Zeng W, Jia Z, et al. (2020) Phosphorus species transformation and recovery without apatite in FeCl3-assisted sewage sludge hydrothermal treatment. *Chem Eng J* 399: 125735. https://doi.org/10.1016/j.cej.2020.125735
53. Huang R, Tang Y (2016) Evolution of phosphorus complexation and mineralogy during (hydro)thermal treatments of activated and anaerobically digested sludge: Insights from sequential extraction and P K-edge XANES. *Water Res* 100: 439–447. https://doi.org/10.1016/j.watres.2016.05.029
54. Wang Y, Lin Y, Chiu PC, et al. (2015) Phosphorus release behaviors of poultry litter biochar as a soil amendment. *Sci Total Environ* 512–513: 454–463. https://doi.org/10.1016/j.scitotenv.2015.01.093
55. Christel W, Bruun S, Magid J, et al. (2014) Phosphorus availability from the solid fraction of pig slurry is altered by composting or thermal treatment. *Bioresour Technol* 169: 543–551. https://doi.org/10.1016/j.biortech.2014.07.030
56. Thygesen AM, Wernberg O, Skou E, et al. (2011) Effect of incineration temperature on phosphorus availability in bio-ash from manure. *Environ Technol* 32: 633–638. https://doi.org/10.1080/09593330.2010.509355
57. Cantrell KB, Hunt PG, Uchimiya M, et al. (2012) Impact of pyrolysis temperature and manure source on physicochemical characteristics of biochar. *Bioresour Technol* 107: 419–428. https://doi.org/10.1016/j.biortech.2011.11.084

AIMS Press